Electronic Supplementary Material (ESI) for Polymer Chemistry.

Non-steady Scaling Model for the Kinetics of the Photo-Induced Free Radical Polymerization of Crosslinking Networks

_____

Patrice Roose,* Evelien Vermoesen and Sandra Van Vlierberghe

_____

Dr. Patrice Roose, allnex Belgium SA/NV, Anderlechtstraat 33, Drogenbos, B-1620, Belgium

Evelien Vermoesen, Prof. Dr. Sandra Van Vlierberghe

Polymer Chemistry and Biomaterials Group, Center of Macromolecular Chemistry, Department of Organic and Macromolecular Chemistry, Krijgslaan 281, Building S4-Bis, Ghent, B-9000, Belgium.

E-mail: patrice.roose@allnex.com

SUPPORTING INFORMATION

SI-1: Schematic representation of the synthesis and the structure of AUP-2

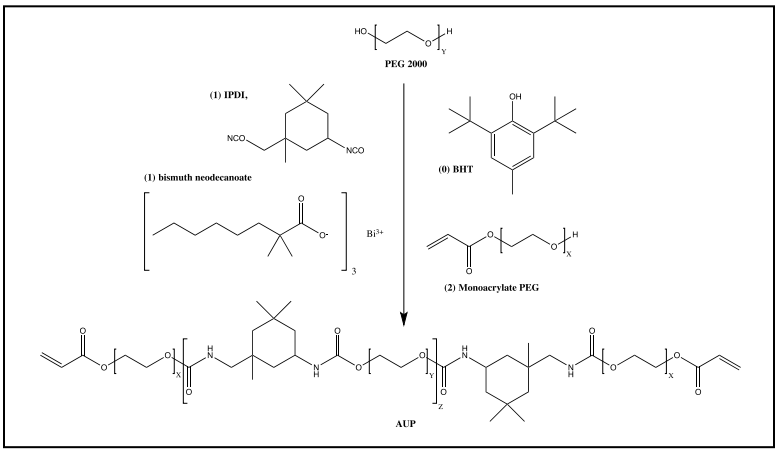

The synthetic procedure for the preparation of the acrylated urethane-based polyethylene glycol precursor (AUP-2) is described here. Briefly, poly(ethylene glycol) (Mn ≈ 2000 g mol^{-1}, Sigma) was reacted with isophorone diisocyanate (BASF) at 75 °C in a 1:2 stoichiometric ratio using 300 ppm of bismuth neodecanoate (Shepherd) as catalyst. In a second step, monoacrylated PEG (Bisomer PEA 6, GEO Specialty Chemicals UK Ltd.) was added along with 300 ppm of bismuth neodecanoate. The temperature was held at 80 °C until a residual isocyanate value < 0.02 mmol g^{-1} was achieved, as determined by potentiometric titration. An acrylic double bond content of 0.595 mmol g^{-1} was measured experimentally by proton NMR spectroscopy.

SI-2: Crystallization and fusion thermograms

The AUP resins were characterized by conventional differential calorimetry using a heat-flux DSC (Mettler DSC823e). Aluminum crucibles of 20 µL were used after an alkaline treatment of the surface using a solution of concentrated NaOH (0.5 M) in order to achieve a regular and reproducible wetting of the pan by the hydrophilic precursors. The sample mass was typically between 2.0 and 3.0 mg forming a layer with a thickness less than 200 µm. All measurements were conducted using dry nitrogen as inert flow gas (50 mL min-1). The temperature and heat flow signal of the DSC cell (Mettler, FRS5) were calibrated using indium. The material was molten at 60°C and then cooled at controlled rate of -5°C min^{-1} to a temperature of -20°C and left for 10 min in isothermal conditions at -20°C. The thermograms of the precursors upon heating at 10 °C min^{-1} are shown in Fig. SI-2.

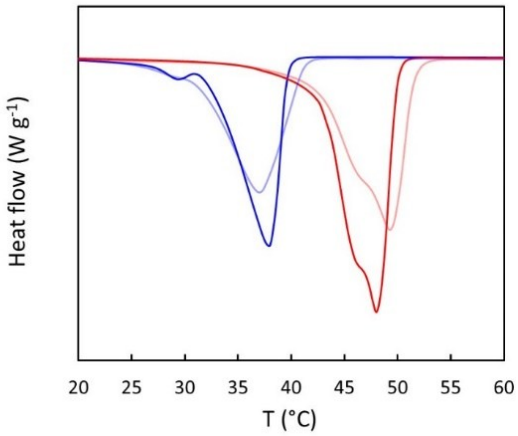

Figure SI-2. DSC thermograms upon heating at a rate of 10°C min^{-1} after the dynamic cooling step and an additional isothermal period of 10 min. Blue: AUP-2; red: AUP-4. The soft lines show the thermograms for the precursors mixed with 0.5 w/% of HCPK as external photoinitiator.

SI-3: Differential Photocalorimetry: Signal handling

With empty crucibles, exposure to UV light for a period of time leads to a smeared heat signal owing to an unbalanced irradiation contribution mixed to the instrumental response. As shown in Fig. SI-3a (left), the input signal generated by opening the shutter of the light source for a predefined period outputs as a delayed or smeared step function due to the convolution with the instrumental response $R(t)$ in the time domain, i.e.

$$H_{out}(t) = H_{in}(t) * R(t)$$

where $H_{in}(t)$ is the undistorted heat flow signal. According to the Gans and Nahman approach (W. L. Gans and N. S. Nahman, IEEE Trans. Instrum. Meas., 1982, 31, 97), a step-like function is transformed in a periodic function by adding the inverted signal at the end of the step period. Upon discrete Fourier transformation of the time domain signal the spectrum is recovered by retaining the data at odd frequencies (Fig. SI-3a right) and with the aid of the convolution theorem, $H_{out}(\omega) = H_{in}(\omega).R(\omega)$, the spectrum of the response function can be extracted and reverted to the time domain by an inverse FT. Fig. SI-3a (left) shows an example of a typical heat flow shift recorded by the DSC upon instantly opening the shutter of the light source with an empty crucible. The overall response function has a shape which can be approximated by the form $y(t) \div t^{\alpha}e^{-\beta t}$ with $\alpha = 2.68$ and $\beta = 1.51$. When the sample crucible is loaded with a photoreactive precursor, the heat flow contribution of the polymerization reaction adds to the underlying background signal upon exposure to UV light as shown in Fig. SI-3b (left). The signal in its periodic form according to Gans-Nahman. The right side of Fig. SI-3b shows the original (blue) and the corrected (red) heat flow signals during the first minutes of the photopolymerization.

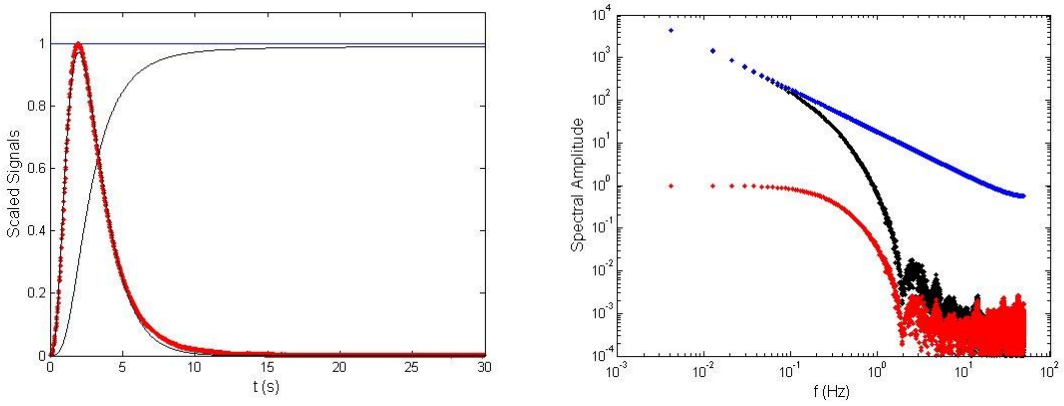

Figure SI-3a. Scaled heat flow signal (black line) recorded by DSC upon exposure of an empty (treated) aluminum crucible to UV-light. The exposure period starts at time zero and the differential heat flow shows a smeared output compared to the undistorted step input (constant blue line) as a result of the instrumental response. The spectra corresponding to the time signals on the left side are shown on the right with the same colors. The instrumental response function (red) is recovered by spectral division and subsequent inverse Fourier transformation, as explained in the text.

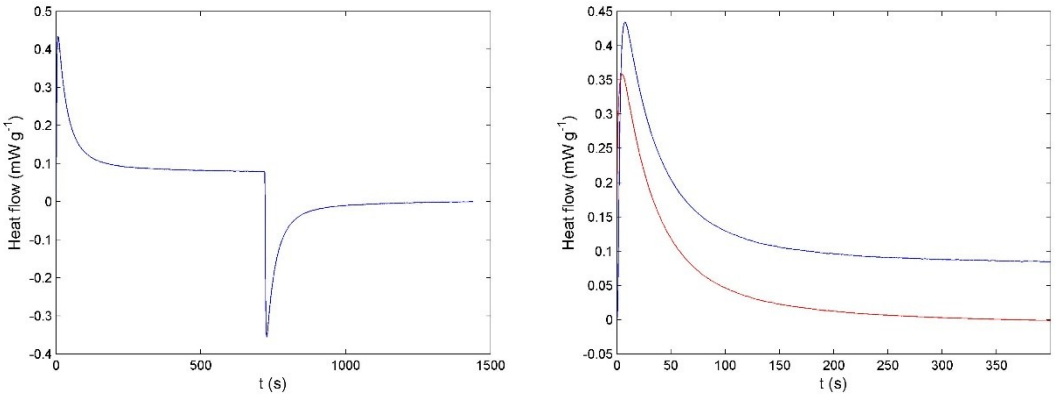

Figure SI-3b. Left: Original heat flow signal for a sample of AUP-4 upon UV exposure for 12 min. Also shown is the inverted signal added in the following 12 min according to the procedure of Gans-Nahman in order to transform the step-like function in a periodic one. Right. The original (blue) and corrected (red) heat flow signals following the approach described before.

SI-4: Error analysis of the model parameters in a non-linear least-squares estimation problem: Minimum variance bound.

The parameter estimation problems were solved by minimizing the least-squares estimator defined as

$$\chi^2 = \sum_{i=1}^{N} \left[\left(y_i - \hat{y}_i \right) / \sigma_i \right]^2$$

where $\hat{y}(\theta)$ is a model function of a set of n adjustable parameters θ. $\{y_i, i = 1,...,N\}$ and $\{\sigma_i, i = 1,...,N\}$ represent the set of N experimental data points and the respective uncertainties measured for the independent variable x_i. Note that $\hat{y}_i = \hat{y}(x_i, \theta)$. In the assumption of equal error, the weighting factors $(1/\sigma_i)^2$ are omitted in the χ^2 function (similar to $\sigma_i = 1$).
The solutions of the NLLS problems were obtained iteratively according to the Levenberg-Marquardt algorithm (Matlab optimization toolbox), resulting in the set of adjusted parameters θ_{ls}.
In contrast to the linear problem, the covariance matrix of the model parameters is not readily determined in the non-linear case. Hence, error analysis is commonly handled in terms of the Cramér-Rao inequality which states that a lower bound for the error covariance matrix of any unbiased estimator of θ is provided by the inverse of the Fisher information matrix J, also referred to as the curvature (or Hessian) matrix in the least-squares case, with elements reading as $J_{jk} = \frac{1}{2} \frac{\partial^2 \chi^2}{\partial \theta_j \partial \theta_k}$. Thus, a reasonable estimate of the error variances for the model parameters is obtained from the diagonal elements of J^{-1} evaluated at $\theta = \theta_{ls}$ (also referred to as the "minimum variance bound"). The standard deviations the read as $\sigma_{\theta_j} = \sqrt{(J^{-1})_{jj}}$.
With unknown uncertainties for the data points, an unbiased estimate is provided from the sample variance of the fit, i.e. $s^2 = \frac{\chi^2(\sigma_i = 1)}{N - n}$, where $\chi^2(\sigma_i = 1)$ is the value of the χ^2 function for $\sigma_i = 1$.
Finally the parameter errors are obtained as $\sigma_{\theta_j} = s\sqrt{(J^{-1})_{jj}}$, evaluated at $\sigma_i = 1$. The parameter errors quantify the significance of the model parameters in a fit and reflect how well they are determined. Correlations between parameters lead to shallow minima within the multiparametric space of the cost function and inflates the elements of J^{-1}, and hence, the parameter errors. The level of correlation is readily established from the non-diagonal elements.

References:

1 P. R. Bevington, Data Reduction and Error Analysis for the Physical Sciences, McGraw-Hill, New York, 1969.
2 H. W. Sorenson, Parameter Estimation: Principles and Problems, Marcel Dekker, New York, 1980.

SI-5: Limiting conversions

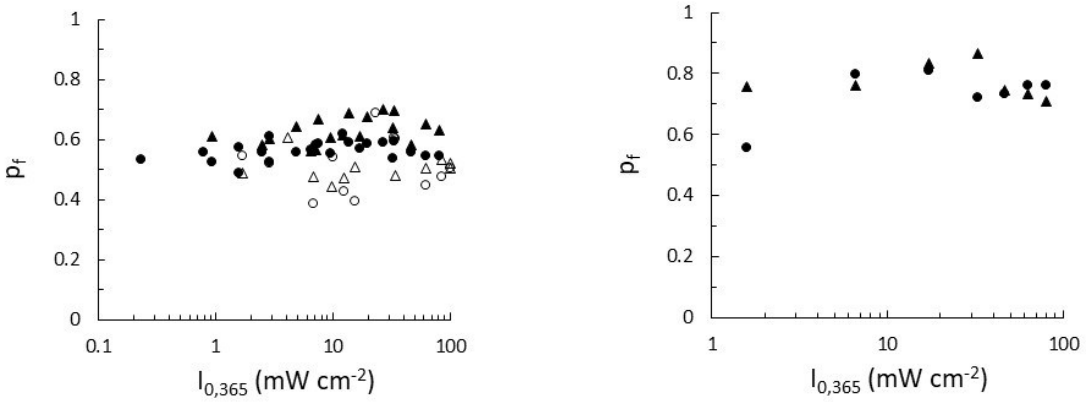

Figure SI-5. The limiting conversion at the end of polymerization vs. incident light intensity at 20 (left) and 60°C (right). The open and solid symbols refer to the photopolymerization kinetics in without and with external PI, respectively, with triangles for AUP-2 and circles for AUP-4.